Environmental Science
Processes & Impacts

Reactions of Chlorinated Ethenes with Surface-Sulfided Iron Materials: Reactivity Enhancement and Inhibition Effects

Journal:	*Environmental Science: Processes & Impacts*
Manuscript ID	EM-ART-12-2019-000593.R1
Article Type:	Paper

Environmental Significance Statement

There is a growing interest in the subject of sulfur-modified iron (ZVI) materials for reductive dehalogenation in recent years owing to its ability to remarkably increase the rates of trichloroethene (TCE) degradation and more selective electron transfer to target contaminants against background constituents. This study examined systematically the effects of different sulfidation treatments on the reactivity of four commercially available ZVIs for reductive dechlorination of perchloroethene (PCE), TCE, and *cis*-dichloroethene (*cis*-DCE). We showed for the first time that the effect of sulfidation is highly contaminant-specific with the observed kinetic enhancements in the order of TCE > PCE > *cis*-DCE. Furthermore, there is a clear divide in *cis*-DCE dechlorination performance among the high-purity ZVIs and those derived from a less pure feedstock such as cast iron. The innate impurities in the latter can serve as adventitious catalysts and their actions are inhibited by sulfidation.

Reactions of Chlorinated Ethenes with Surface-Sulfided Iron Materials: Reactivity Enhancement and Inhibition Effects

Syful Islam[1,^], Yanlai Han[1,^,#], Weile Yan[1,2*]

[1]Department of Civil, Environmental and Construction Engineering, Texas Tech University, Texas, United States

[2]Department of Civil and Environmental Engineering, University of Massachusetts Lowell, Massachusetts, United States

^ with equal contribution

Current affiliation: U.S. EPA National Exposure Research Laboratory

* Corresponding author. Tel: (978)-934-2256

Email address: weile_yan@uml.edu

Abstract

Recent studies on the use of controlled sulfur amendment to improve the reactivity and selectivity of zerovalent iron (ZVI) in reductive dechlorination reactions have generated a renewed interest in ZVI-based remediation materials. However, existing studies have focused on the reactions between trichloroethene (TCE) and lab-synthesized ZVI, the applicability of sulfidation to ZVIs with different material characteristics for reductive dechlorination of chloroethenes such as tetrachloroethene (PCE) and *cis*-dichloroethene (cis-DCE) have not been systematically examined. In this study, four ZVI materials from commercial sources having different size, morphological, and compositional characteristics were subject to various sulfidation treatments and were assessed in batch reactions with PCE, TCE, or *cis*-DCE. Sulfur-amendment induces modest increases in PCE degradation and steers reaction to a cleaner pathway that has minimum accumulation of partially dechlorinated intermediates. In the case of *cis*-DCE, bifurcating outcomes were observed that include enhancement effects for two high-purity ZVIs and inhibitory effects for two ZVIs possessing low levels of metal impurities. Further investigations based on controlled metal dosing reveal that the trace metals commonly present in cast iron or recycled metal scraps, such as Cu and Ni, can act as adventitious catalysts for *cis*-DCE reduction. Sulfidation results in poisoning of these catalytic ingredients and accounts for the adverse effect observed with a subset of ZVIs. Collectively, this study confirms enhanced degradation of highly chlorinated ethenes (PCE and TCE) by sulfidation of ZVIs from diverse origins; nonetheless, the effects of sulfidation can be highly variable for the lesser chlorinated ethenes due to differences in the material characteristics of ZVI and the predominant dechlorination pathways.

Keywords: ZVI, sulfur, sulfidation, dechlorination, TCE, PCE, and *cis*-DCE

Introduction

Chlorinated ethenes, such as tetrachloroethene (PCE) and trichloroethene (TCE), are common groundwater pollutants and their efficient removal remains a lingering challenge due to their historical uses in diverse industries [1, 2], significant accumulation in fractured bedrocks or low-permeability media [3, 4], and recalcitrance to natural attenuation [1, 5]. In addition to TCE and PCE, lesser chlorinated analogues such as *cis*-dichloroethene (*cis*-DCE), 1,1- dichloroethene (1,1-DCE), and vinyl chloride (VC) have been frequently detected in the subsurface environment owing to incomplete biodegradation [6] or the formation of intermediates during abiotic transformation [7, 8]. These complications have spurred continuous search for effective remediation approaches in the past three decades.

Zero-valent iron (ZVI or Fe(0)) materials have been applied extensively to environmental remediation [6, 9-13]. The nanoscale or bulk ZVI materials can transform chlorinated ethenes into non-toxic end products with minimal build-up of problematic intermediates, however, one serious drawback is the tendency of iron to passivate in groundwater matrices or under aerobic conditions [14-18]. In recent years, a collection of studies have shown that amending the iron substrate with low doses of sulfur significantly mitigates passivation and steering the electron selectivity towards the target contaminants [19-24]. In addition to these desirable properties, the promise of ZVI sulfidation lies in the simplicity and robustness of the sulfidation process. In general, controlled sulfidation can be attained by either exposing ZVI to aqueous or gaseous sulfur precursors [19, 20, 24] or placing ZVI in contact with solid phase sulfur (e.g., elemental sulfur) using mechanochemical means

[25, 26], and concise summaries of a variety of sulfidation protocols are available in several recent reviews [6, 27]. Our earlier investigation demonstrated that at low sulfur doses, improvements in TCE reduction rates attained by different sulfur precursors are comparable. Further, the enhancement effect saturates at a S/Fe mole ratio of ca. 0.05 for the nanoscale ZVI, thus a consistent beneficial outcome is expected over a wide range of operation conditions [22].

Reduction of chlorinated ethenes by iron substrates may occur via direct electron transfer or indirect reduction involving atomic hydrogen [6, 28]. Concerning the mechanisms of sulfur-induced improvements in TCE dechlorination rates, multiple accounts have been proposed including depassivation of the native oxide layer [29], more facile electron conductance from the Fe(0) core to contaminants via the iron sulfide phase (FeS_x) [23, 30, 31], and increased availability of atomic hydrogen on the particle surface [22]. An unequivocal conclusion cannot be made at this time due to differences in experimental conditions (e.g., in dilute vs. saturated TCE solutions), as the dominant mechanism may shift with solution pH and TCE concentration [28]. Furthermore, there is evidence that the enhancement effect is reactant-specific [6, 31, 32], and the outcome of sulfidation may not necessarily manifest in the same way for different contaminants. With this, we recognize that the majority of the studies reported thus far have employed lab-synthesized iron (nano)particles and used TCE as the target contaminant. These studies do not consider the complexity in actual remediation systems, including the variations in physicochemical characteristics and processing history of different ZVI reagents deployed in the field and the presence of co-contaminants and reaction intermediates in contamination plumes. As such, whether sulfidation can serve as a general

strategy to improve the performance of in situ chemical reduction (ISCR) is not fully assessed.

In this study, we investigated sulfidation of four bulk ZVI materials, including ZVI prepared from an electrolytic method or reduction of Fe-carbonyl complexes and two commercial ZVI products frequently employed for environmental remediation. Sodium thiosulfate was used as the sulfur precursor following our previous protocol [22]. The rates and reaction products of the resultant iron materials with PCE, TCE, and *cis*-DCE were systematically assessed. PCE and TCE are parent contaminants, while *cis*-DCE is a persistent daughter product arising during biological attenuation of TCE/PCE plumes [3, 6]. The goals of these investigations were to assess the applicability of sulfidation as a general approach to engineering the reactive properties of pre-formed ZVI materials, to evaluate the effects of sulfur amendment on the rates and daughter product formation during degradation of common chlorinated ethenes detected in the subsurface, and to highlight the advantages and potential complications of sulfidation for *in situ* reductive dechlorination applications.

MATERIALS AND METHODS

Chemicals and Materials

Four types of commercial ZVI were used in this study. Alfa Aesar iron powder (catalogue # AA0017030) was purchased from Fisher Chemical. BASF carbonyl iron powder (CIP-OM), was provided by BASF SE (Germany). Hepure Ferox-PRB^{TM} iron powder was supplied by Hepure Technologies Inc (Hillsborough, NJ, USA). Peerless cast iron powder

(50D) was provided by Peerless Metal Powders & Abrasive (Detroit, MI, USA). The materials were designated in short as ZVI^{AA}, ZVI^{CIP}, ZVI^{HP} and ZVI^{PL}, respectively. Among the materials, ZVI^{PL} and ZVI^{HP} are widely used commercial ZVI materials for active remediation of chlorinated solvent-impacted sites. Unlike the two high-purity ZVI of synthetic origins (ZVI^{AA} and ZVI^{CIP}), the remediation-grade ZVIs were manufactured from cast iron stock. ZVI^{HP} was specifically developed for permeable reactive barrier applications and therefore has a relatively large size distribution. To improve its size uniformity, the particles were sieved, and only the fraction passing through the ASTM Sieve #40 (opening size 425 μm) was collected for further evaluations. Other ZVI materials were used without size fractionation.

Pretreatment and Sulfidation of ZVI

All surface treatments were conducted in the atmospheric environment. Deoxygenated distilled-deionized water (DDI) was used in laboratory procedures. Deoxygenation of DDI was carried out by purging the solutions with N_2 for 30 min prior to its use. In all aqueous treatments or reductive dechlorination experiments, the loading of ZVI in the aqueous phase was 10 g/L, except for ZVI^{HP}, which was used at 50 g/L due to its relatively large particle size (Table 1). Each material was subject to the following sulfidation treatments. Method one, referred to as *direct sulfidation*, entails the addition of an appropriate amount of sodium thiosulfate ($Na_2S_2O_3$) to an aqueous suspension of ZVI, and the mixture was agitated on a wrist action shaker for 60 min at 250 rpm. The resultant particles were collected via vacuum filtration using 0.2 μm membrane filters (PALL life sciences), rinsed with deoxygenated DDI, and used immediately in the dechlorination

experiments. The second method, dubbed *two-step sulfidation*, involves pre-washing the commercial ZVI with 0.1% v/v HCl for 1 h (or 0.1% v/v acetic acid in the case of ZVI^{CIP}) to remove the surface passivation layer. Dilute acetic acid was employed for ZVI^{CIP} due to its higher efficiency at stripping off the organic surface coating on the CIP particles. The acid washed particles were collected through vacuum filtration, rinsed with DDI, and were re-dispersed in DDI. Following that, thiosulfate was amended following the same procedures as the direct sulfidation process. Unless otherwise noted, the amount of thiosulfate added corresponds to a S/Fe mole ratio of 0.05. 1 mole of thiosulfate is considered to release 1 mole of sulfide ion [22, 33]. As a comparison, the iron receiving the acid washing but not sulfidation was also prepared and evaluated for its dechlorination efficiency.

Preparation of Metal-amended ZVI

To assess the effects of trace metal impurities on the reactivity of the as-is and sulfur-amended iron materials, ZVI^{CIP} (a ZVI with no detectable metal impurities) was deposited with a small amount of Cu, Ni, or Mn. Metal amendment was performed by pre-washing 300 mg ZVI^{CIP} in 30-mL dilute acetic acid for 24 h. The particles were harvested by vacuum filtration and immediately immersed in 30 mL of 150 mg/L Cu(II), Ni(II), or Mn(II) solution (refer to Chemicals in SI for the metal salts used) and mixed on a wrist-action shaker at 250 rpm for 1 h. The resultant particles were collected by vacuum filtration & rinsed with DDI. A portion of these particles was used immediately in dechlorination experiments, and the remaining particles were subject to the two-step sulfidation following the same procedure as described in the earlier text, and the resultant particles were used immediately in further experiments. The filtrates were analyzed by inductively coupled plasma-mass spectrometry

(ICP-MS) and the mass loading of Cu, Ni, and Mn in the respective particles were determined to be 0.14 (± 0.01) %, 0.11 (± 0.07) %, and 0.19 (± 0.04) %, respectively.

Reduction of Chlorinated Ethenes

TCE, PCE, and *cis*-DCE degradation experiments were performed to evaluate the effects of different surface treatments on the dechlorination performance of various ZVIs. All batch experiments were carried out in 45-mL EPA vials containing 30 mL of aqueous solution and the remaining as headspace. ZVI materials were introduced into deoxygenated solution at 10 g/L except for ZVI^{HP}, which was loaded at 50 g/L. Each reactor was capped with a PTFE-lined mininert valve, and a small aliquot of the stock solution of TCE, PCE, or *cis*-DCE in methanol was injected to start the experiment. Periodically, an aliquot (25 - 50 μL) of the headspace gas was withdrawn using a gastight syringe and was analyzed for the parent and daughter compounds.

Analytical methods

A gas chromatography (GC) system (Agilent 6890) equipped with an Agilent PoraPlot Q column (25 m x 0.32 mm) and a flame ionization detector (FID) was used to quantify the parent compounds and reaction products. The headspace samples were injected in a splitless mode at 250°C. The oven temperature (35°C for 5 min, ramp 12°C/min to 220°C, and hold at 220°C for 5 min) provided adequate separation between chlorinated ethenes and all reaction products. The calibration curves for TCE, PCE, and *cis*-DCE were constructed by headspace analysis of the respective aqueous standard solutions prepared in the same vials as the experimental reactors. Calibrations for hydrocarbons (C_1-C_6) were

performed using the commercial gas standards after accounting for partition between headspace and aqueous phases using the respective Henry's Law constants [34, 35].

Material Characterizations

The average particle sizes of the ZVI materials were measured using an API Aerosizer Particle Size Analyzer (TSI Inc, Massachusetts, USA). The specific surface areas were analyzed with a surface area and pore size analyzer (Quantachrome NOVA 2000e, USA) using 11-point N_2-adsorption curves. Metal impurities in ZVI materials were quantified by digesting the as-received ZVI particles in 5.6% (v/v) HCl solution for 72 h. The resultant solution was filtered, and the filtrate was analyzed using ICP-MS. The digestion was performed in duplicates.

Results and Discussion

Characteristics of ZVI Materials

Table 1 summarizes the properties of the ZVI materials employed in this study. The SEM images of the particles are available in Fig. S1 in the Supporting Information. ZVI^{AA} and ZVI^{CIP} exhibited a similar morphology of a spherical shape with smooth, non-porous surface texture that is consistent with their syntheses routes of electrolytic reduction and thermal decomposition of iron pentacarbonyl ($Fe(CO)_5$) [36]. In comparison to the uniform morphology of the synthetic ZVIs, the two ZVIs used in environmental remediation, i.e., ZVI^{HP} and ZVI^{PL}, appeared as flaky and irregular-shaped particles. ZVI^{HP} comprised predominantly of coarse granules spanning several tens to hundreds of microns in diameter

and the particle surface was characterized by a high degree of roughness contributed by crevices and cracks. ZVI^{PL} had a broad size distribution ranging from very fine (< 10 μm) particles to large chunky flakes spanning tens of microns. Although the SEM images of ZVI^{PL} suggest mainly coarse granules, the surface-area-weighted average size determined through the Aerosizer method is 3.3 ± 2.5 μm, which reflects the dominant quantity of small particles as the Aerosizer method operates on a particle counting principle [37]. Both ZVI^{HP} and ZVI^{PL} displayed a tiered structure with the surface of the primary particles decorated with a large number of fine debris (insets of Fig. S1). This feature has been observed of the mechanically processed ZVI [38], and it may account for the relatively high specific surface areas of the two materials (Table 1) in spite of the large primary particle sizes revealed in the SEM micrographs (Fig. S1).

The purity of ZVI reported by the manufacturers suggests that ZVI^{AA} has the highest purity, followed by ZVI^{CIP}. The two remediation-grade ZVIs carry up to 10 wt.% impurities (Table 1). To identify the major non-ferrous metal constituents in the solid matrix, all ZVI materials were digested in 6% (v/v) hydrochloric acid solution for 72 h. Neither ZVI^{AA} or ZVI^{CIP} contains detectable levels of metal ingredients other than Fe. ZVI^{HP} and ZVI^{PL} have 0.48 wt.% and 0.67 wt.% manganese, respectively. Other metals of a significant presence include copper and nickel (Table 1). Both materials generated appreciable amounts of solid residues upon acid digestion (Fig. S2). No attempt was made to ascertain the composition of these residues, although carbon, silicon, and sulfur ingredients are expected based on their common presence in cast iron-derived ZVI reagents [39, 40].

Effect of Sulfidation on Reduction of TCE

Reductive dechlorination of TCE was conducted using the as-received ZVIs and those that had received various treatments including: (a) dilute acid washing, (b) direct sulfidation, and (c) two-step sulfidation. The adoption of acid washing prior to sulfidation is based on the rationale that the affinity of low-valent sulfur ligands for iron oxide surfaces are significantly lower than for the metal iron [41], therefore, the presence of a continuous layer of native oxide may impede sulfidation of the metal phase. The rates of TCE degradation by the original and surface treated ZVIs are depicted in Figure 1. As shown, the reactivity of the as-received ZVIs varies considerably. The two remediation ZVIs were considerably more reactive than the synthetic iron (i.e., ZVI^{AA} and ZVI^{CIP}) as the latter group did not produce a significant loss of TCE during a 30-day monitoring period. Although direct exposure to thiosulfate led to noticeable increases in TCE dechlorination rates, the combination of acid washing and sulfur amendment delivered the greatest rate enhancement effects consistently for ZVI^{AA} and ZVI^{CIP}.

Comparatively, acid washing alone elicited remarkable increases in TCE reaction rates for ZVI^{PL} and ZVI^{HP}, indicating that the surfaces of the two ZVIs are fairly susceptible to chemical modification and these materials may be inherently more reactive than the high-purity ZVIs. Compared to acid-washing, direct or two-step sulfur amendments gave rise to small incremental improvements for ZVI^{HP}, yet the same treatments substantially accelerated TCE decomposition by ZVI^{PL}. The highest rate constants attained by sulfur treated ZVI^{PL} and ZVI^{HP} were 190 folds and 4.2 folds of the as-received materials, respectively.

To assess the effect of S/Fe ratio, sulfidation of ZVI^{PL} was performed using the two-step sulfidation procedure but with varying doses of thiosulfate. As plotted in Fig. 2, a steep

rise in the surface-normalized TCE decomposition rate constant (k_{SA}) was observed at a S/Fe mole ratio as low as 0.0037, corresponding to 670 μM of thiosulfate in contact with 10 g/L ZVI^{PL} suspension. The rate constant plateaus as S/Fe ratio exceeds *ca.* 0.01. This trend resembles the characteristics of a similar plot of the sulfidated nZVI (S-nZVI), although in the latter case, rate saturation occurs at a nominal S/Fe mole ratio of approximately 0.05 [22, 30]. The smaller dose of sulfur precursor required by these micron-sized ZVI to attain the saturated reaction rate is likely related to a smaller specific surface area available of the ZVI granules relative to the nanoparticles. For both types of iron, the observation that the reactivity of the particles initially increased with the sulfur loading then leveled out at higher sulfur loadings demonstrates that the enhancement effect is a surface phenomenon. Excessive sulfur, either present in the aqueous phase or forming surface-attached or discrete sulfide particles, did not contribute appreciably to the observed reaction rates. The finding also implies that the natural level of sulfide in an anoxic environment may be adequate to improve ZVI performance *in situ*.

Product distribution data (Fig. 4b), determined at ca. 90% conversion or the last sampling point for experiments with slow kinetics, indicates that the major products of TCE reactions with different ZVIs were acetylene, ethene, ethane, and higher order hydrocarbons (only C_3 to C_6 hydrocarbons were quantified). Chlorinated intermediates were not detected during TCE experiments. Except for acetylene, whose concentration peaked at an intermediate stage (Fig. S3), other products appeared to accumulate in the system without further reactions. Comparing the product distribution profiles across the types of ZVI and the treatment methods, it was observed that sulfidation of iron resulted in an increased proportion

of acetylene relative to other products. The shifts in product distribution are more prominent in the case of ZVI^{HP} and ZVI^{PL}. Regardless of the ZVI origin, the two-step sulfidation led to greater dominance of acetylene compared to direct sulfidation. In prior studies of TCE reaction with ZVI [42], iron sulfides [43-45], or sulfidated nanoscale ZVI [22, 30], significant accumulation of acetylene was also reported and a direct conversion of TCE to acetylene as opposed to stepwise hydrogenolysis was inferred. Prior kinetic analysis shows that the increased production of acetylene is mainly attributed to a large boost in the rate of TCE to acetylene conversion, whereas the hydrogenation reactions of acetylene are not affected or moderately slowed down by sulfidation [22]. Therefore, sulfur amendment improves multiple reductive steps to varying extents and the initial conversion of TCE to acetylene exhibits the most pronounced enhancement effect.

Effect of Sulfidation on Reduction of Other Chlorinated Ethenes

The effect of sulfur amendment was assessed for the dechlorination of PCE and *cis*-DCE. Among DCE isomers, *cis*-DCE is the most persistent and tends to accumulate in the environment during natural attenuation of PCE or TCE [6, 46]. The surface area-normalized rate constants (k_{SA}) of different ZVIs are compared in Figure 3. For consistency, the acid-washed (as opposed to as-received) particles were used as the reference materials to eliminate the effect of varying degrees of passivation caused by material storage or handling. The sulfidated particles were all subject to the two-step sulfidation. With sulfur amendment, more rapid PCE dechlorination was consistently observed of all ZVIs (Figures 3a). The rate constants of the sulfur-laden ZVIs were in the range of 140% to 630% of those of the acid-treated particles,

with the two remediation-grade ZVIs (i.e., ZVI^{PL} and ZVI^{HP}) exhibiting the largest gains in reaction rates. However, the extents of improvements for PCE were somewhat smaller than TCE (Figure 3b). The variations in sulfidation-induced enhancement effects may stem from the difference in reductive dechlorination pathways undertaken by different chlorinated ethenes [43, 45, 47]. As shown in Figure 4a, PCE decomposition by acid-washed ZVI^{AA} and ZVI^{CIP} yielded a significant amount of TCE and higher order hydrocarbons. Upon sulfur treatment, TCE accumulation was virtually eliminated. For the two remediation-grade ZVI (ZVI^{HP} and ZVI^{PL}), TCE production was minimal by either acid-treated or sulfur-amended particles. Sulfidation of the latter two types of ZVI also created remarkable increases in acetylene formation. Other intermediates, including dichloroethenes or vinyl chloride, were not detected in the product mix.

Prior studies reported that abiotic dehalogenation of chloroethenes proceeds via hydrogenolysis, which goes by sequential replacement of chlorine substituents by hydrogen producing lesser chlorinated intermediates, or alternatively, the parent compound may chemisorb onto iron surface and the surface complex undergoes concerted C-Cl bond dissociation to yield acetylene as the main intermediate [43, 44, 47-49]. In either case, reduction via either direct electron transfer or indirectly through surface-adsorbed atomic hydrogen are involved [6, 22, 23, 28]. Electrochemical investigations suggest that the contribution of the two pathways to PCE and TCE decomposition varies with contaminant concentration and solution pH [28]. Direct electron transfer is thought to occur to a larger degree for PCE reduction than TCE at near neutral pH [28, 47]. Recent investigations have shown that, in contrast to the large improvement in TCE dechlorination performance, sulfidation has little or inconsistent effect

on the reduction of carbon tetrachloride [6, 22], which reacts predominantly via direct electron transfer. As such, the modest enhancement in PCE degradation seen in this study implies indirect reduction with atomic hydrogen may play a less important role in PCE reduction than in the case of TCE [28], in agreement with findings from computational analysis that electron transfer to PCE on ZVI surface involves a smaller activation energy than TCE [50].

In comparison to PCE and TCE experiments, in which sulfur amendment is able to bring about faster dechlorination for all iron materials, sulfidation resulted in bifurcating outcomes for *cis*-DCE reactions (Figure 3c). Specifically, sulfidation of ZVI^{AA} and ZVI^{CIP} produced more swift *cis*-DCE reduction compared to their acid-washed counterparts, rendering over an order of magnitude increase in k_{SA} for both ZVI^{AA} and ZVI^{CIP}. Therefore, for these two synthetic ZVIs, sulfidation is proven advantageous for the degradation of all chloroethenes evaluated in this work. Nonetheless, sulfur treatment casts a pronounced inhibitory effect on the other two ZVI materials, causing 66% and 98% decreases in the rate constants for ZVI^{HP} and ZVI^{PLS}, respectively. *cis*-DCE may lose one chlorine generating vinyl chloride as an intermediate or it may shed off two chlorines concertedly to yield acetylene or its hydrogenation products [46, 47]. We did not detect vinyl chloride in the product mixture in all *cis*-DCE experiments and there was no consistent changes in product distribution related to sulfur treatments (Fig. 4c). Although a smaller enhancement effect by sulfidation is expected of *cis*-DCE as the structure of the molecule is cumbersome for the elimination of the two chlorine substituents concurrently [48], we could not rationalize the drastic loss of reactivity due to sulfidation for the two ZVIs intended for remediation use (ZVI^{HP} and ZVI^{PL}). Instead, we

hypothesize that the metal impurities present in these two ZVI materials may influence the outcomes of sulfidation treatments. This hypothesis was tested with the following study.

Effects of Metal Impurities and Sulfur Amendment

Cu, Ni, and Mn were detected in the bulk substrate of ZVI^{HP} and ZVI^{PL} at up to 0.7 wt.% (Table 1). To investigate whether these trace metals may fortuitously catalyze dehalogenation, we used ZVI^{CIP}, a high-purity ZVI with no detectable metal impurities, as the base material and loaded it individually with a small amount of Cu, Ni, or Mn via aqueous impregnation. The mass loadings of Cu, Ni, and Mn in the particles were reported in the Materials and Methods section. These values are comparable to the impurity content of the two commercial ZVI materials (Table 1). We reckon that, although the artificially impregnated particles likely bear all impurities on the surface whereas impurities in ZVI^{HP} and ZVI^{PL} are expected to distribute throughout the particles, the former can provide meaningful insights into the effects of individual metals in the commercial ZVIs.

Among the trace metals incorporated onto ZVI^{CIP}, Mn had a negligible effect on *cis*-DCE degradation efficiency (Figure 5a). Ni-deposited particles exhibited highly variable performance between replicate experiments, possibly due to slow transformation of Ni(II) to its catalytic active form on ZVI surface based on findings in our prior studies [51, 52]. Comparatively, the Cu-amended particles were the most efficient at *cis*-DCE dechlorination. k_{SA} of Cu-amended ZVI^{CIP} is 6.6 x 10^{-5} L/m^2•min, approximately 200 times the rate constant of the acid-washed ZVI^{CIP} or 15 times that of the sulfidated ZVI^{CIP} (Table 2). Compared to Ni or Pd, Cu is not an efficient hydrogenation catalyst, but Cu is fairly active for the dissociation

of carbon-halogen bonds [53, 54]. Combining ZVI and Cu can therefore enable rapid conversion of TCE to predominantly ethene. However, when the particles deposited with Cu were exposed to thiosulfate solution, the catalytic effect imparted by Cu was largely annihilated (Figure 5b). The product distribution pattern indicates that the dominant products of Cu-amended ZVI^{CIP} (viz., ethene and a smaller amount of ethane) were replaced with predominantly higher-order hydrocarbons when the Cu-amended particles underwent sulfur treatment (Fig. S4), suggesting the activity of the surface Cu sites was silenced. Sulfur poisoning of transition metal catalysts have been extensively studied [41, 55-57]. The strong chemisorption of sulfur onto metal surfaces causes perturbation of the electronic structures of the metal atoms, reconstruction of surface structures, and blocking of active sites, leading to severe attenuation of catalytic activities [41, 57]. Although sulfur deactivation of Cu-amended ZVI materials for reductive dechlorination has not been specifically examined, poisoning of Pd-amended ZVI, a model catalytic bimetallic material for hydrodechlorination reactions, by aqueous reduced sulfur species (sulfide, sulfite, or thiol groups in natural organic matter) has been noted in prior studies [58-60]. The potent ability of the aqueous sulfur precursor to poison the adventitious catalysts on the two remediation-grade ZVIs (i.e., ZVI^{HP} and ZVI^{PL}) may explain for the drastic decrease in *cis*-DCE degradation rates upon sulfidation of these impure ZVIs.

A similar investigation using PCE as the starting compound shows that the deposition of Cu (or Ni to a smaller effect) onto the ZVI surface led to more rapid PCE transformation, with k_{SA} increasing by 35 folds for the Cu-amended particles relative to the acid-washed particles (Fig. 5c). Exposing the Cu-amended ZVI to aqueous thiosulfate resulted in a greatly attenuated PCE conversion rate, nonetheless the remnant reactivity of the particles was still

higher than that of the acid-washed but unamended particles (Fig. 5d). In the headspace mixture, TCE accounted for 41% of the total products when the Cu-amended particles were used, in contrast to minimal TCE accumulation using the sulfidated ZVI or ZVI receiving Cu-deposition followed by sulfidation (Fig. S4). This implies an important role of Cu in controlling the reduction pathways and also agrees with a recent finding that the reaction of TCE with Cu-Fe bimetallic creates substantial amounts of chlorinated intermediates that were not observed with pristine or sulfidated nZVI [23].

It is interesting to note that, while PCE and *cis*-DCE reduction rates by Cu-amended ZVI^{CIP} exceed that of the sulfidated particles, the addition of Cu exerts only a moderate enhancement effect on TCE reaction (Table 2). Further, comparing the rates of Cu-amended ZVI^{CIP} against the same particles receiving Cu amendment followed by sulfidation, the loss of reactivity due to sulfidation is the most pronounced for *cis*-DCE, followed by PCE and TCE, respectively. These results imply that the catalytic function of Cu is more important for *cis*-DCE degradation than that those of the highly chlorinated ethenes. On the other hand, with reference to pure unamended ZVI, sulfidation brings about a remarkably higher degree of reactivity improvement for TCE than PCE and *cis*-DCE. The compounded outcome of the enhancing and inhibitive actions of sulfur for the remediation grade ZVI would be that sulfidation should result in an overall improved TCE degradation performance and a certain degree of reactivity loss in *cis*-DCE dechlorination. This is consistent with the observations made of ZVI^{PL} and ZVI^{HP}. It is postulated that Cu catalyzes direct dissociative dechlorination, but has a minor impact on pathway involving activated hydrogen species. The varied outcomes

caused by the sulfidation of Cu-laden ZVI therefore reflect the contribution of different reduction mechanisms for different chloroethenes as summarized in Figure 6.

Conclusions

Recent studies have investigated sulfidation of laboratory synthesized nanoscale ZVI using either pre-synthesis or post-synthesis sulfidation procedures [19, 20, 22]. Whether sulfidation is applicable to a wide spectrum of ZVI materials would have crucial implications for the amenability of this technique to *in situ* remediation applications. The results obtained in this study confirm that sulfur amendment is applicable to commercially available ZVI to attain greater dechlorination efficiencies for the highly chlorinated ethenes, with the enhancement effect being more pronounced for TCE than PCE. The preparation of sulfur-amended ZVI using bottom-up synthesis methods is therefore not necessary. As predicted previously [22], a low level of sulfur in the solid phase is adequate to achieve the saturated enhancement effect, which suggests *in situ* sulfidation using naturally available or augmented sulfur source is feasible for ZVI that had been emplaced in the fields. This can be a potentially important tool to reinstate the performance of previously installed iron materials and to sustain the beneficial effect of sulfidation considering that the surface-residing sulfur species is susceptible to oxidation in an oxic environment.

While sulfidation brings about more rapid and complete dehalogenation of PCE and TCE across all forms of ZVIs evaluated in this work, there are significant differences in the *cis*-DCE dechlorination efficiencies, suggesting subtle variations in the ZVI composition due

to different material origins and processing routes can profoundly affect iron reactive properties. With the two high-purity ZVIs, sulfidation is beneficial for the degradation of all chlorinated ethenes evaluated in this study. In contrast, the ZVI materials intended for remediation saw marked loss of reactivity towards *cis*-DCE due to poisoning of metal impurities that act as adventitious catalysts. As the ZVI materials used in the environmental applications are frequently sourced from mixed industrial feedstock or recycled scrap metals, trace levels of impurities are expected. The distinct effects of common impurities such as Cu in facilitating the reduction of *cis*-DCE and its susceptibility to sulfur poisoning point to several practical considerations. For instance, the application of sulfur-modified iron may be more suitable for source zone mitigation than treating plumes that have undergone extensive environmental aging, as the latter may contain significant levels of partially dechlorinated intermediates. On the other hand, the inclusion of common impurities (due to recycled nature of the iron substrate) may make ZVI more efficient at transforming the lesser chlorinated intermediates. More broadly, the findings in this study demonstrate interesting interactions among iron, sulfur, and metal impurities that play out the many facets of ZVI chemistry. The ability to manipulate these factors would enable rational design and use of ZVI materials from diverse sources to create more tailored solutions to sites with complex mixture of contaminants.

Acknowlegement

The authors acknowledge the start-up fund by TTU and funding support from the National Science Foundation (CHE-1611465). The authors thanks the ZVI suppliers (BASF, Hepure

Technologies, and Peerless MPA) for providing the iron samples and the assistance by Dr. Juliusz Warzywoda for particle size and surface area analyses.

Supporting Information

SEM images of commercial ZVIs, product evolution during TCE degradation by various ZVI^{PL}, and the distribution of products of PCE and *cis*-DCE reactions with metal-amended or metal-amendment-followed-by-sulfidation ZVI^{CIP} are avaialble in the supporting information. The Supporting Information is available free of charge on the ACS Publications website.

References

1. P. L. McCarty, *Groundwater Contamination by Chlorinated Solvents: History, Remediation Technologies, and Strategies*, 2010.
2. M. J. Moran, J. S. Zogorski and P. J. Squillace, Chlorinated solvents in groundwater of the United States, *Environmental Science & Technology*, 2007, **41**, 74-81.
3. H. F. Stroo, A. Leeson, J. A. Marqusee, P. C. Johnson, C. H. Ward, M. C. Kavanaugh, T. C. Sale, C. J. Newell, K. D. Pennell, C. A. Lebron and M. Unger, Chlorinated Ethene Source Remediation: Lessons Learned, *Environmental Science & Technology*, 2012, **46**, 6438-6447.
4. R. A. Freeze and D. B. McWhorter, A framework for assessing risk reduction due to DNAPL mass removal from low-permeability soils, *Ground Water*, 1997, **35**, 111-123.
5. H. F. Stroo, M. Unger, C. H. Ward, M. C. Kavanaugh, C. Vogel, A. Leeson, J. A. Marqusee and B. P. Smith, Remediating chlorinated solvent source zones, *Environmental Science & Technology*, 2003, **37**, 224A-230A.
6. D. M. Fan, Y. Lan, P. G. Tratnyek, R. L. Johnson, J. Filip, D. M. O'Carroll, A. N. Garcia and A. Agrawal, Sulfidation of Iron-Based Materials: A Review of Processes and Implications for Water Treatment and Remediation, *Environmental Science & Technology*, 2017, **51**, 13070-13085.
7. C. M. Su and R. W. Puls, Kinetics of trichloroethene reduction by zerovalent iron and tin: Pretreatment effect, apparent activation energy, and intermediate products, *Environmental Science & Technology*, 1999, **33**, 163-168.
8. T. L. Johnson, M. M. Scherer and P. G. Tratnyek, Kinetics of halogenated organic compound degradation by iron metal, *Environmental Science & Technology*, 1996, **30**, 2634-2640.
9. D. O'Carroll, B. Sleep, M. Krol, H. Boparai and C. Kocur, Nanoscale zero valent iron and bimetallic particles for contaminated site remediation, *Advances in Water Resources*, 2013, **51**, 104-122.
10. A. B. Cundy, L. Hopkinson and R. L. Whitby, Use of iron-based technologies in contaminated land and groundwater remediation: A review, *Science of the total environment*, 2008, **400**, 42-51.
11. X. Zhao, W. Liu, Z. Q. Cai, B. Han, T. W. Qian and D. Y. Zhao, An overview of preparation and applications of stabilized zero-valent iron nanoparticles for soil and groundwater remediation, *Water Research*, 2016, **100**, 245-266.
12. R. A. Crane and T. B. Scott, Nanoscale zero-valent iron: Future prospects for an emerging water treatment technology, *Journal of Hazardous Materials*, 2012, **211**.
13. W. Yan, H.-L. Lien, B. E. Koel and W.-x. Zhang, Iron nanoparticles for environmental clean-up: recent developments and future outlook, *Environmental Science-Processes & Impacts*, 2013, **15**, 63-77.
14. K. Ritter, M. S. Odziemkowski and R. W. Gillham, An in situ study of the role of surface films on granular iron in the permeable iron wall technology, *Journal of Contaminant Hydrology*, 2002, **55**, 87-111.
15. V. Sarathy, P. G. Tratnyek, J. T. Nurmi, D. R. Baer, J. E. Amonette, C. L. Chun, R. L. Penn and E. J. Reardon, Aging of iron nanoparticles in aqueous solution: Effects on structure and reactivity, *Journal of Physical Chemistry C*, 2008, **112**, 2286-2293.
16. J. E. Martin, A. A. Herzing, W. Yan, X.-q. Li, B. E. Koel, C. J. Kiely and W.-x. Zhang, Determination of the oxide layer thickness in core-shell zerovalent iron nanoparticles, *Langmuir*, 2008, **24**, 4329-4334.

17. J. Klausen, P. J. Vikesland, T. Kohn, D. R. Burris, W. P. Ball and A. L. Roberts, Longevity of granular iron in groundwater treatment processes: Solution composition effects on reduction of organohalides and nitroaromatic compounds, *Environmental Science & Technology*, 2003, **37**, 1208-1218.
18. J. Farrell, M. Kason, N. Melitas and T. Li, Investigation of the long-term performance of zero-valent iron for reductive dechlorination of trichloroethylene, *Environmental Science & Technology*, 2000, **34**.
19. S. R. C. Rajajayavel and S. Ghoshal, Enhanced reductive dechlorination of trichloroethylene by sulfidated nanoscale zerovalent iron, *Water Research*, 2015, **78**, 144-153.
20. E.-J. Kim, J.-H. Kim, A.-M. Azad and Y.-S. Chang, Facile Synthesis and Characterization of Fe/FeS Nanoparticles for Environmental Applications, *Acs Applied Materials & Interfaces*, 2011, **3**, 1457-1462.
21. D. Fan, G. O. Johnson, P. G. Tratnyek and R. L. Johnson, Sulfidation of Nano Zerovalent Iron (nZVI) for Improved Selectivity during In- Situ Chemical Reduction (ISCR), *Environmental Science & Technology*, 2016, 9558-9565.
22. W. Yan and Y. Han, Reductive Dechlorination of Trichloroethene by Zero-valent Iron Nanoparticles: Reactivity Enhancement through Sulfidation Treatment, *Environmental Science & Technology*, 2016, **In press** DOI: 10.1021/acs.est.1026b03997.
23. F. He, Z. J. Li, S. S. Shi, W. Q. Xu, H. Z. Sheng, Y. W. Gu, Y. H. Jiang and B. D. Xi, Dechlorination of Excess Trichloroethene by Bimetallic and Sulfidated Nanoscale Zero-Valent Iron, *Environmental Science & Technology*, 2018, **52**, 8627-8637.
24. A. N. Garcia, H. K. Boparai and D. M. O'Carroll, Enhanced Dechlorination of 1,2-Dichloroethane by Coupled Nano Iron-Dithionite Treatment, *Environmental Science & Technology*, 2016, **50**, 5243-5251.
25. Y. W. Gu, B. B. Wang, F. He, M. J. Bradley and P. G. Tratnyek, Mechanochemically Sulfidated Microscale Zero Valent Iron: Pathways, Kinetics, Mechanism, and Efficiency of Trichloroethylene Dechlorination, *Environmental Science & Technology*, 2017, **51**, 12653-12662.
26. J. Z. Jiang, R. K. Larsen, R. Lin, S. Morup, I. Chorkendorff, K. Nielsen, K. Hansen and K. West, Mechanochemical synthesis of Fe-S materials, *Journal of Solid State Chemistry*, 1998, **138**, 114-125.
27. J. X. Li, X. Y. Zhang, Y. K. Sun, L. P. Liang, B. C. Pan, W. M. Zhang and X. H. Guan, Advances in Sulfidation of Zerovalent Iron for Water Decontamination, *Environmental Science & Technology*, 2017, **51**, 13533-13544.
28. J. Wang and J. Farrell, Investigating the role of atomic hydrogen on chloroethene reactions with iron using tafel analysis and electrochemical impedance spectroscopy, *Environmental Science & Technology*, 2003, **37**, 3891-3896.
29. Y. Xie and D. M. Cwiertny, Use of Dithionite to Extend the Reactive Lifetime of Nanoscale Zero-Valent Iron Treatment Systems, *Environmental Science & Technology*, 2010, **44**, 8649-8655.
30. S. Bhattacharjee and S. Ghoshal, Optimal Design of Sulfidated Nanoscale Zerovalent Iron for Enhanced Trichloroethene Degradation, *Environmental Science & Technology*, 2018, **52**, 11078-11086.
31. J. Xu, Y. Wang, C. Weng, W. Bai, Y. Jiao, R. Kaegi and G. V. Lowry, Reactivity, Selectivity, and Long-Term Performance of Sulfidized Nanoscale Zerovalent Iron with Different Properties, *Environmental Science & Technology*, 2019, **53**, 5936-5945.

32. M. Mangayayam, K. Dideriksen, M. Ceccato and D. J. Tobler, The Structure of Sulfidized Zero-Valent Iron by One-Pot Synthesis: Impact on Contaminant Selectivity and Long-Term Performance, *Environmental Science & Technology*, 2019, **53**, 4389-4396.
33. M. Kappes, G. S. Frankel, N. Sridhar and R. M. Carranza, Reaction Paths of Thiosulfate during Corrosion of Carbon Steel in Acidified Brines, *Journal of the Electrochemical Society*, 2012, **159**, C195-C204.
34. C. L. Yaws, *Yaws' Handbook of Thermodynamic and Physical Properties of Chemical Compounds*, McGraw-Hill (accessed through Knovel), 2003.
35. *CRC Handbook of Chemistry and Physics, 76th ed.*, CRC Press, Boca Raton, FL, 1996.
36. BASF, The CIP Technology - How is carbonyl iron powder manufactured?, https://www.dispersions-pigments.basf.com/portal/basf/em/dt.jsp?setCursor=1_827912, (accessed Last accessed Jan 2, 2019).
37. J. Thornburg, S. J. Cooper and D. Leith, Counting efficiency of the API Aerosizer, *Journal of Aerosol Science*, 1999, **30**, 479-488.
38. S. Li, W. Yan and W.-x. Zhang, Solvent-free production of nanoscale zero-valent iron (nZVI) with precision milling, *Green Chemistry*, 2009, **11**, 1618-1626.
39. Hepure Technologies Inc., Technical Specification Sheet Ferox-Flow™ ZVI Reactive Iron Powder.
40. NAVFAC, Permeable Reactive Barrier Cost and Performance Report, TR-NAVFAC-ESC-EV-1207, 2012.
41. J. A. Rodriguez and J. Hrbek, Interaction of sulfur with well-defined metal and oxide surfaces: Unraveling the mysteries behind catalyst poisoning and desulfurization, *Accounts of Chemical Research*, 1999, **32**, 719-728.
42. H. Song and E. R. Carraway, Catalytic hydrodechlorination of chlorinated ethenes bly nanoscale zero-valent iron, *Applied Catalysis B-Environmental*, 2008, **78**, 53-60.
43. E. C. Butler and K. F. Hayes, Kinetics of the transformation of trichloroethylene and tetrachloroethylene by iron sulfide, *Environmental Science & Technology*, 1999, **33**, 2021-2027.
44. E. C. Butler and K. F. Hayes, Factors influencing rates and products in the transformation of trichloroethylene by iron sulfide and iron metal, *Environmental Science & Technology*, 2001, **35**, 3884-3891.
45. H. Y. Jeong, H. Kim and K. F. Hayes, Reductive dechlorination pathways of tetrachloroethylene and trichloroethylene and subsequent transformation of their dechlorination products by mackinawite (FeS) in the presence of metals, *Environmental Science & Technology*, 2007, **41**, 7736-7743.
46. H. Y. Jeong, K. Anantharaman, Y.-S. Han and K. F. Hayes, Abiotic Reductive Dechlorination of cis-Dichloroethylene by Fe Species Formed during Iron- or Sulfate-Reduction, *Environmental Science & Technology*, 2011, **45**, 5186-5194.
47. W. A. Arnold and A. L. Roberts, Pathways and kinetics of chlorinated ethylene and chlorinated acetylene reaction with Fe(O) particles, *Environmental Science & Technology*, 2000, **34**, 1794-1805.
48. A. L. Roberts, L. A. Totten, W. A. Arnold, D. R. Burris and T. J. Campbell, Reductive elimination of chlorinated ethylenes by zero valent metals, *Environmental Science & Technology*, 1996, **30**, 2654-2659.
49. T. Li and J. Farrell, Reductive dechlorination of trichloroethene and carbon tetrachloride using iron and palladized-iron cathodes, *Environmental Science & Technology*, 2000, **34**, 173-179.

50. D. H. Lim and C. M. Lastoskie, Density Functional Theory Studies on the Relative Reactivity of Chloroethenes on Zerovalent Iron, *Environmental Science & Technology*, 2009, **43**, 5443-5448.
51. X. Q. Li and W. X. Zhang, Iron nanoparticles: the core-shell structure and unique properties for Ni(II) sequestration, *Langmuir*, 2006, **22**, 4638-4642.
52. Y. Han and W. Yan, Bimetallic Nickel-Iron Nanoparticles for Groundwater Decontamination: Effect of Groundwater Constituents on Surface Deactivation, *Water Research* 2014, **66**, 149-159.
53. M. X. Yang, S. Sarkar, B. E. Bent, S. R. Bare and M. T. Holbrook, Degradation of multiply-chlorinated hydrocarbons on Cu(100), *Langmuir*, 1997, **13**, 229-242.
54. V. Y. Borovkov, D. R. Luebke, V. I. Kovalchuk and J. L. d'Itri, Hydrogen-assisted 1,2-dichloroethane dechlorination catalyzed by Pt-Cu/SiO2: Evidence for different functions of Pt and Cu sites, *Journal of Physical Chemistry B*, 2003, **107**, 5568-5574.
55. J. Oudar, Sulfur adsorption and poisoning of metallic catalysts *Catalysis Reviews-Science and Engineering*, 1980, **22**, 171-195.
56. G. A. Somorjai and Y. Li, *Introduction to Surface Chemistry and Catalysis*, Wiley, Hoboken, New Jersey, 2nd edn., 2010.
57. C. H. Bartholomew, Mechanisms of catalyst deactivation, *Applied Catalysis a-General*, 2001, **212**, 17-60.
58. W. L. Yan, A. A. Herzing, X. Q. Li, C. J. Kiely and W. X. Zhang, Structural Evolution of Pd-Doped Nanoscale Zero-Valent Iron (nZVI) in Aqueous Media and Implications for Particle Aging and Reactivity, *Environmental Science & Technology*, 2010, **44**, 4288-4294.
59. F.-D. Kopinke, D. Angeles-Wedler, D. Fritsch and K. Mackenzie, Pd-catalyzed hydrodechlorination of chlorinated aromatics in contaminated waters-Effects of surfactants, organic matter and catalyst protection by silicone coating, *Applied Catalysis B-Environmental*, 2010, **96**, 323-328.
60. K. Mackenzie, H. Frenzel and F. D. Kopinke, Hydrodehalogenation of halogenated hydrocarbons in water with Pd catalysts: Reaction rates and surface competition, *Applied Catalysis B-Environmental*, 2006, **63**, 161-167.

606 Table 1. Properties of Commercial ZVI products investigated in this study

ZVI Product	**Average Diameter (μm)**	**BET Surface Area (m^2/g)[c]**	**Fe content (wt.%)[d]**	**Metal Impurities (wt.%)[e]**		
				Mn	Ni	Cu
Alfa Aesar Iron Powder (ZVI^{AA})	3.80 ± 1.07[a]	0.347 ± 0.001	~ 99.5	N.D.	N.D.	N.D.
BASF CIP™ OM (ZVI^{CIP})	3.33 ± 1.05[a]	0.349 ± 0.003	> 97.8	N.D.	N.D.	N.D.
Hepure Ferox-PRB™ (ZVI^{HP})	< 425 μm[b]	0.407 ± 0.02	> 95%	0.48 ± 0.03	0.032 ± 0.005	0.073 ± 0.009
Peerless 50D (ZVI^{PL})	3.25 ± 2.5[a]	1.95 ± 0.003	> 90%	0.67 ± 0.06	0.19 ± 0.02	0.15 ± 0.02

607 [a] Determined as the surface-area weighted mean diameter using aerosizer. [b] Fraction passing through
608 ASTM Sieve No. 40 (opening size 425 μm) was used in this study. [c] Estimated based on 11-point N_2
609 adsorption curves. [d] Based on specifications provided by manufacturer. [e] Measured via acid digestion
610 and ICP-MS analyses. N.D. stands for below detection limit, which is 0.003%, 0.0002%, and 0.011%
611 for Mn, Ni, and Cu, respectively.

612

Table 2. Surface area-normalized pseudo-first-order rate constants of chlorinated ethene degradation by ZVI^{CIP} receiving various surface treatments

Surface Treatment	Contaminant	k_{SA} ($L \cdot m^{-2} \cdot min^{-1}$)	Carbon Recovery [a]
Acid wash	TCE	N.D. [b]	0.94
Acid wash + sulfidation		1.12 (± 0.36) x 10^{-4}	0.57
Cu-amendment		9.15 x 10^{-5}	1.12
Cu-amendment + sulfidation		2.47 (± 0.06) x 10^{-5}	0.91 (± 0.01)
Acid wash	PCE	3.15 (± 0.11) x10^{-6}	0.81 (± 0.02)
Acid wash + sulfidation		4.49 (± 1.26) x10^{-6}	0.66 (± 0.05)
Cu-amendment		1.12 (± 0.21) x10^{-4}	1.16 (± 0.003)
Cu-amendment + sulfidation		1.09 (± 0.17) x10^{-5}	0.94 (± 0.26)
Acid wash	*cis* -DCE	3.28 (± 2.49) x10^{-7}	0.92 (± 0.02)
Acid wash + sulfidation		4.41 (± 2.10) x10^{-6}	1.07 (± 0.03)
Cu-amendment		6.61 (± 0.59) x10^{-5}	1.08 (± 0.18)
Cu-amendment + sulfidation		8.16 (± 0.20) x10^{-7}	0.93 (± 0.04)

[a] determined at the point of ca. 90% conversion or, for slow reactions, the last sampling point. [b] rate constant not determined due to negligible product formation over 30 days. Numbers in brackets represent standard deviations of replicate experiments.

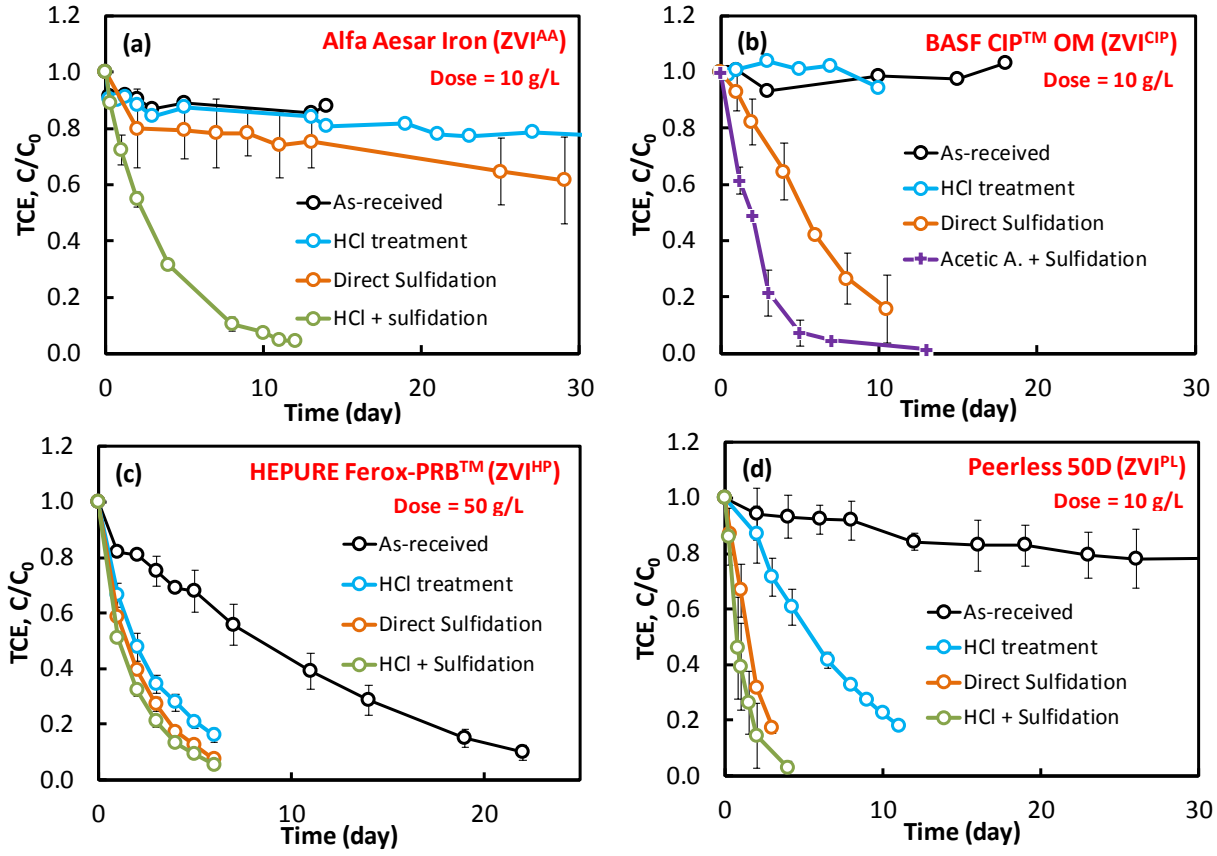

Figure 1. Effects of chemical treatment of various commercial ZVI on TCE degradation rates. TCE initial concentration was 25 mg/L.

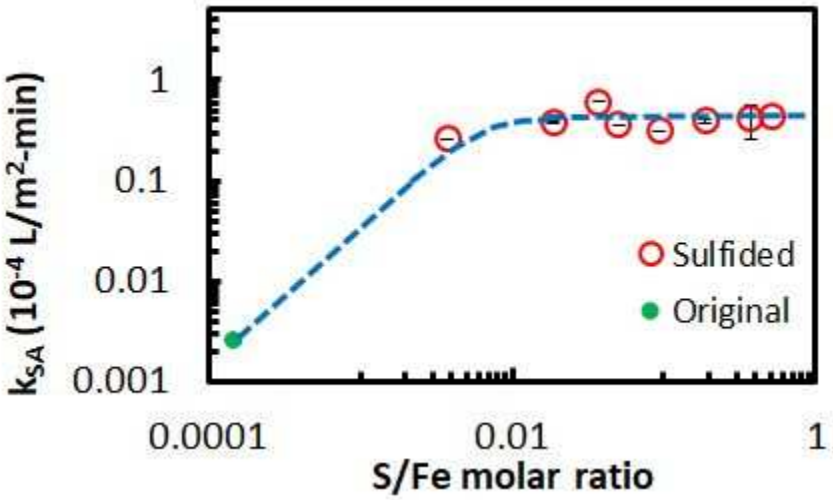

Figure 2. Effect of sulfidation of ZVI^{PL} on TCE degradation rates. TCE initial concentration was 25 mg/L. The loading of iron particles was 10 g/L. Sulfidation of ZVI^{PL} follows the two-step procedure of acid washing followed by immersion in thiosulfate solution.

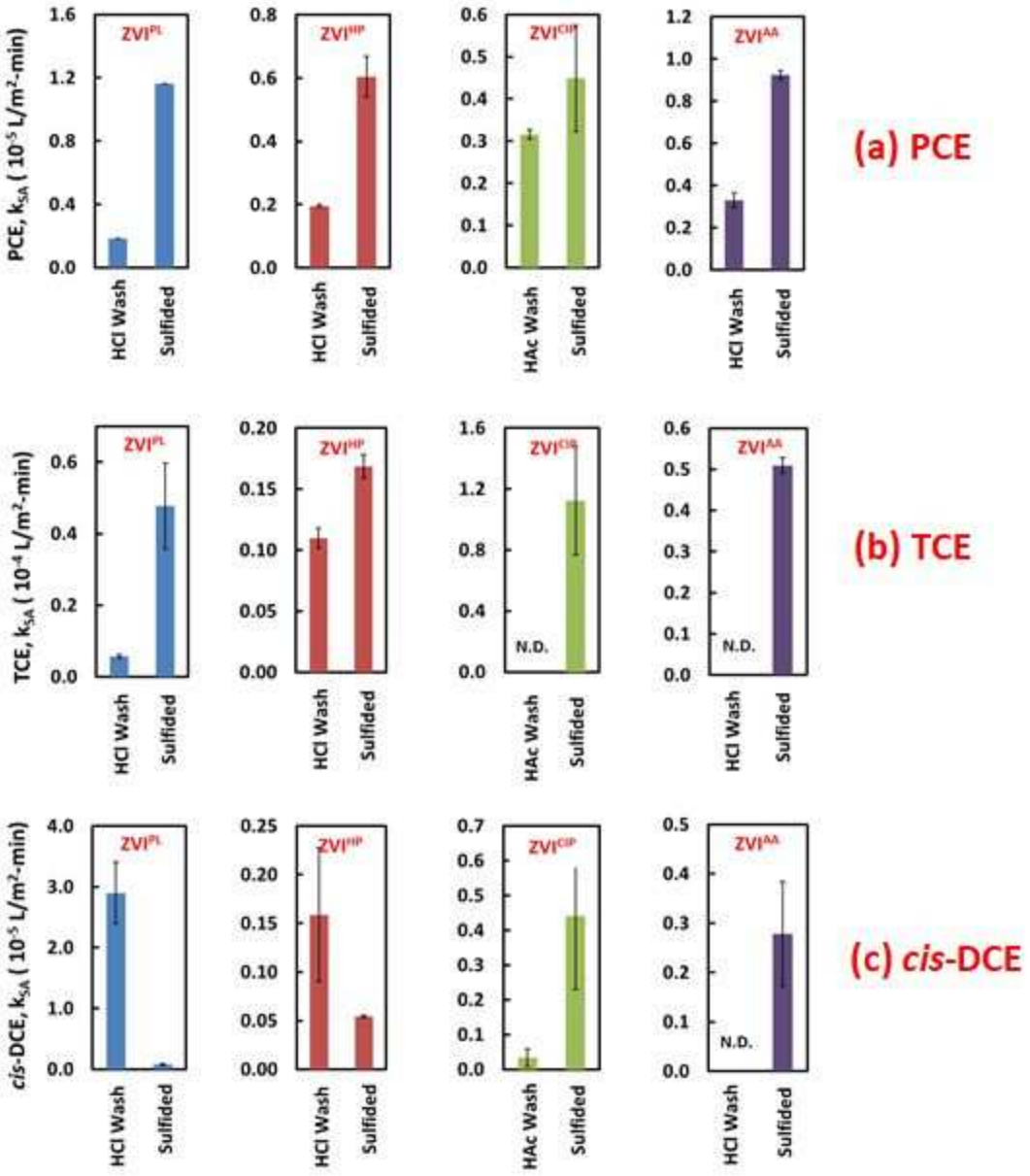

Figure 3. Comparison of the effects of acid treatment and sulfidation on degradation rates of (a) PCE, (b) TCE, and (c) *cis*-DCE by various ZVI materials. Initial concentrations of PCE, TCE, and *cis*-DCE were 0.19 mM. ZVI loadings are the same as those in Figure 1. "N.D." denotes non-detectable due to negligible product formation in the 30-day monitoring periods.

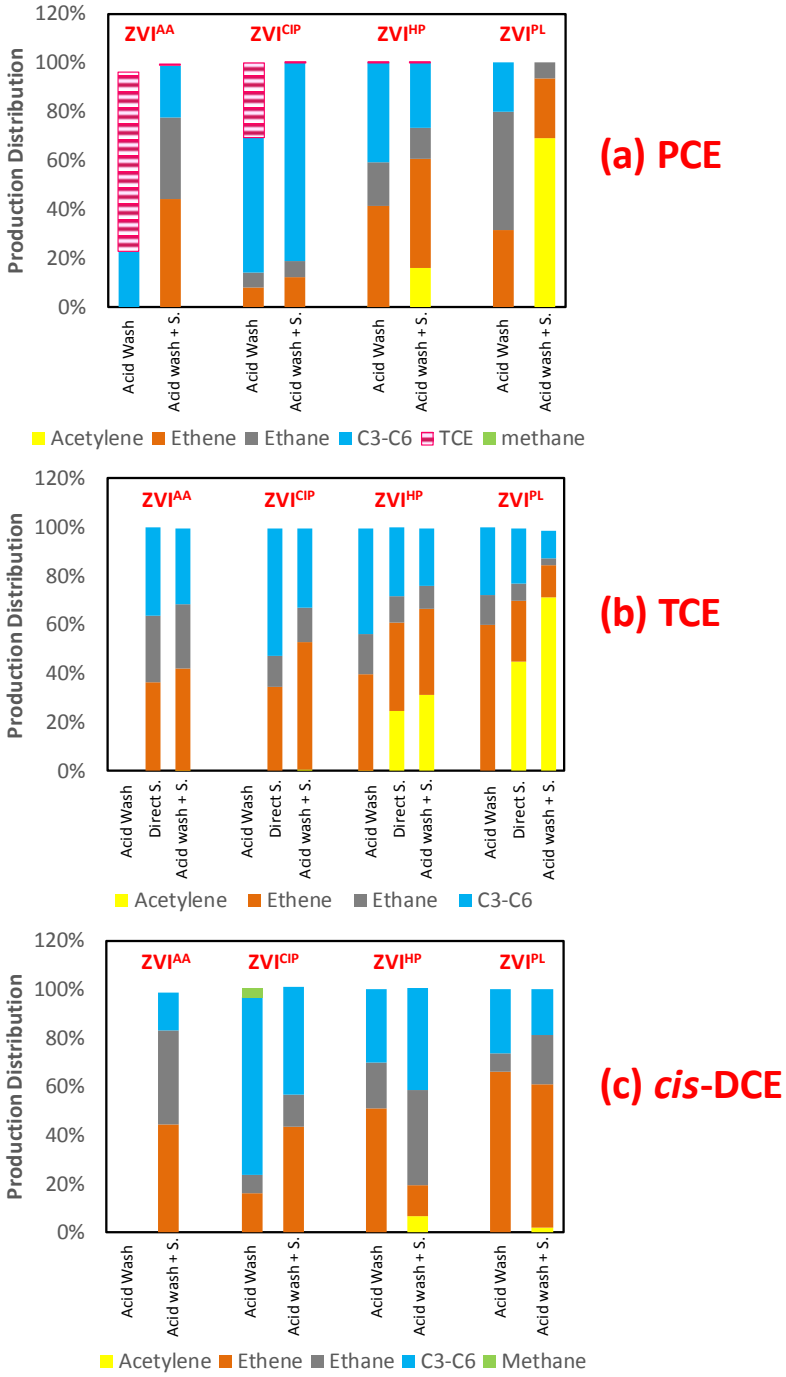

Figure 4. Distribution of reaction products from dechlorination of (a) PCE, (b) TCE, and (c) *cis*-DCE by various ZVI materials. Initial concentrations of PCE, TCE, and *cis*-DCE were 0.19 mM. ZVI loadings are the same as those in Figure 1.

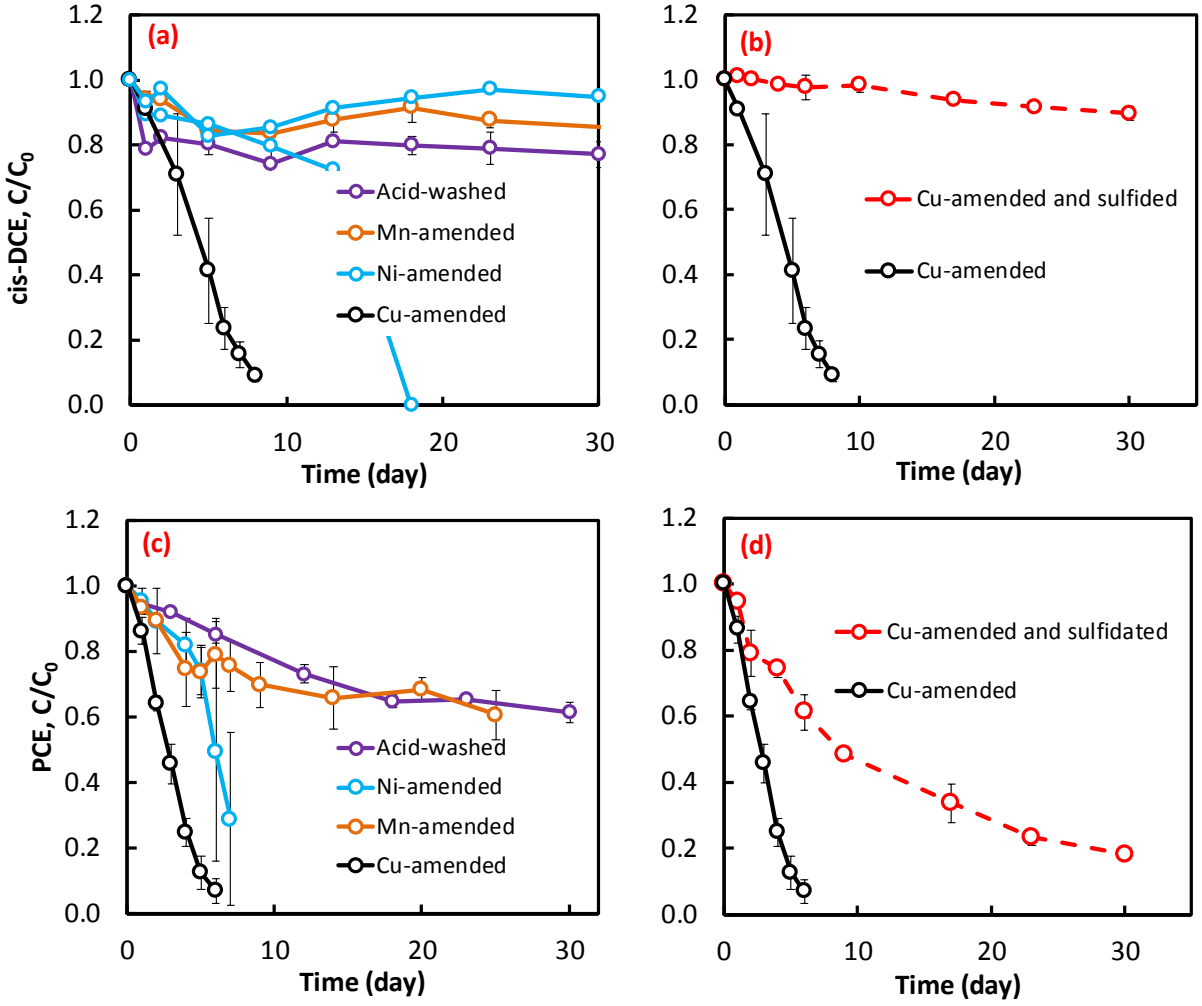

Figure 5. Effect of metal impurities on (a) *cis*-DCE and (c) PCE degradation rates by metal-amended ZVI^{CIP}. Inhibitory effect of sulfidation on (b) *cis*-DCE and (d) PCE degradation by metal-amended ZVI^{CIP}. Initial concentrations of PCE and *cis*-DCE were 0.19 mM. ZVI loading was 10 g/L. Note that duplicate experiments of Ni-amended ZVI^{CIP} were shown separately due to large variations.

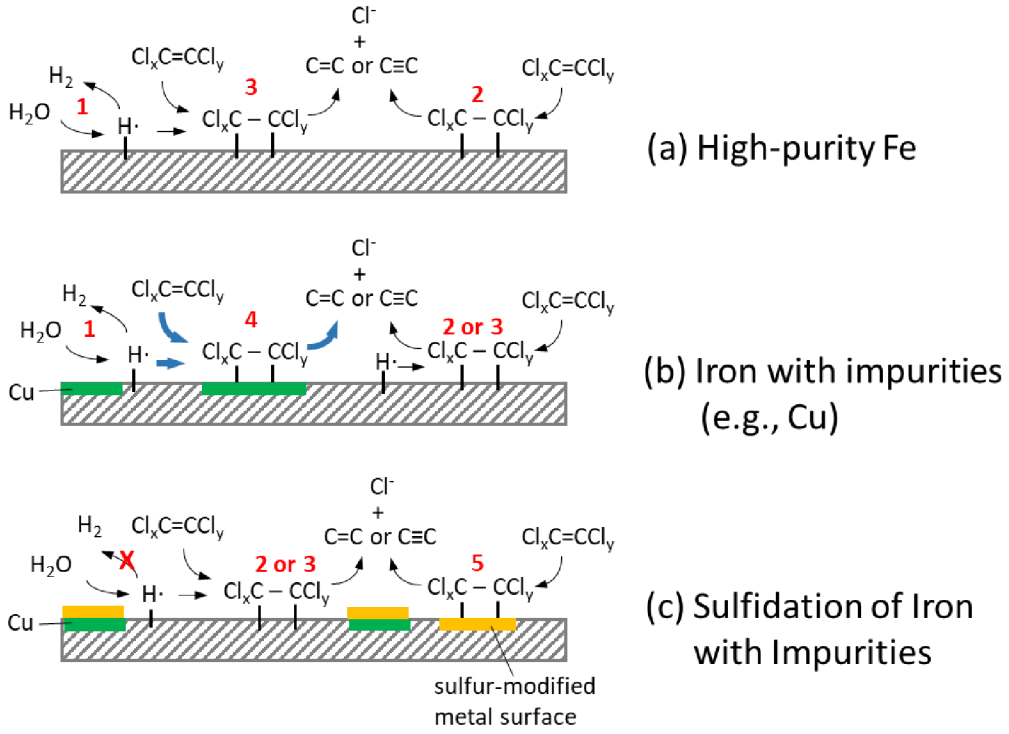

Figure 6. Schematics of reactions of chlorinated ethenes on various iron surfaces. Processes labelled with numbers are 1) water reduction, 2) direct surface dechlorination, 3) dechlorination assisted with atomic hydrogen, 4) catalyzed (hydro)dechlorination on metal impurities (e.g., Cu), 5) FeS-mediated dechlorination. Bold lines represent catalyzed processes.

TOC Graphic

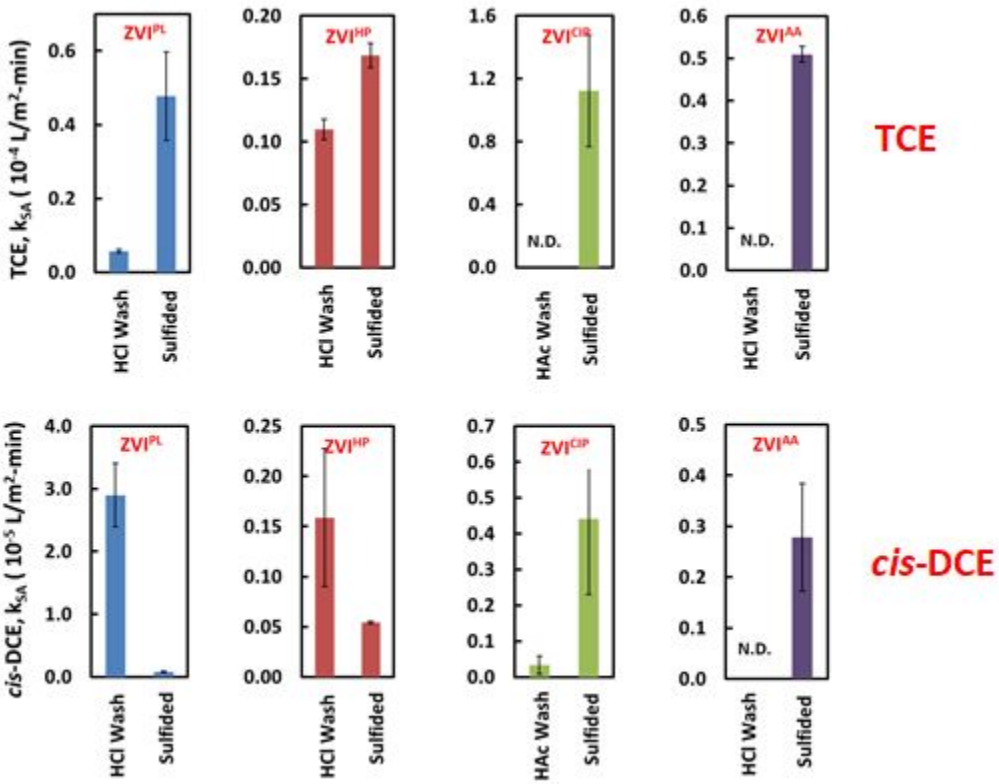
TCE, k_{SA} (10^{-4} L/m^2-min)
ZVI^{PL}
ZVI^{HP}
ZVI^{CIP}
ZVI^{AA}
N.D.
N.D.
HCl Wash
Sulfided
HCl Wash
Sulfided
HAc Wash
Sulfided
HCl Wash
Sulfided
TCE
cis-DCE, k_{SA} (10^{-5} L/m^2-min)
ZVI^{PL}
ZVI^{HP}
ZVI^{CIP}
ZVI^{AA}
N.D.
HCl Wash
Sulfided
HCl Wash
Sulfided
HAc Wash
Sulfided
HCl Wash
Sulfided
cis-DCE